

Photoluminescence engineering using III-V dielectric metamaterials

Sheng Liu^{*(1)}, Sadvikas Addamane⁽²⁾, Michael B. Sinclair⁽¹⁾, Gordon A. Keeler⁽¹⁾, Ganesh Balakrishnan⁽²⁾, and Igal Brener⁽¹⁾

(1) Sandia National Laboratories, Albuquerque, NM, 87185

(2) University of New Mexico, Albuquerque, NM 87185

Abstract

Metamaterials comprising man-made “atoms” have shown great promise for next generation optoelectronic devices. Here we will show that dielectric metamaterials can be used to engineer the photoluminescence of active media that are epitaxially grown inside the metamaterials. We design and fabricate two different kinds of structures: symmetry-broken Fano resonator arrays and regular nano-cylinder resonator arrays. With both designs, we observe large enhancement of the photoluminescence intensities as well as spectral tuning due to the resonantly enhanced electromagnetic fields inside the dielectric resonators and different mode coupling.

1. Introduction

Enormous progress has been achieved in the field of metamaterial research since the first demonstration in 2000 [1]. More recently, all-dielectric metamaterials consisting of arrays of high-index, subwavelength-size Mie resonators have attracted much attention recently due to their much lower loss at optical frequencies compared with their metallic counterparts. Moreover, these Mie resonators interact strongly with both electric and magnetic fields and therefore enable manipulation of the electromagnetic permittivity and permeability. Great success has been achieved in nonlinear optical processes, ultrathin optical components and advanced wavefront engineering using dielectric metamaterials [2-4]. However, most of the work has been done using silicon, which is not an efficient light emitter and lacks second-order nonlinearities due to its centrosymmetric lattice structure.

Recently, our group demonstrated a new class of dielectric metamaterials based upon III-V semiconductors that exhibit large intrinsic optical nonlinearities and allow for full integration with optoelectronic functionality. We experimentally realized multi-layer metamaterials that have remained highly challenging for other material systems and therefore provide a new degree of freedom for device engineering [5]. We also observed resonantly enhanced second harmonic generation (SHG) using our GaAs dielectric resonators [6] that provide nonlinear conversion efficiencies higher than 10^{-5} , which is several orders of magnitude than the SHG efficiency obtained from metallic resonators.

III-V semiconductor based dielectric metamaterials can also be directly employed for improving upon light

emitters due to their direct bandgap properties. Here we show that both the regular nano-cylinder arrays and symmetry-broken Fano resonator arrays can be used to largely enhance the light emission of quantum dots embedded inside the resonators. We also show that the emission peak can be widely tuned within the emission bandwidth of the emitters.

2. Sample preparation

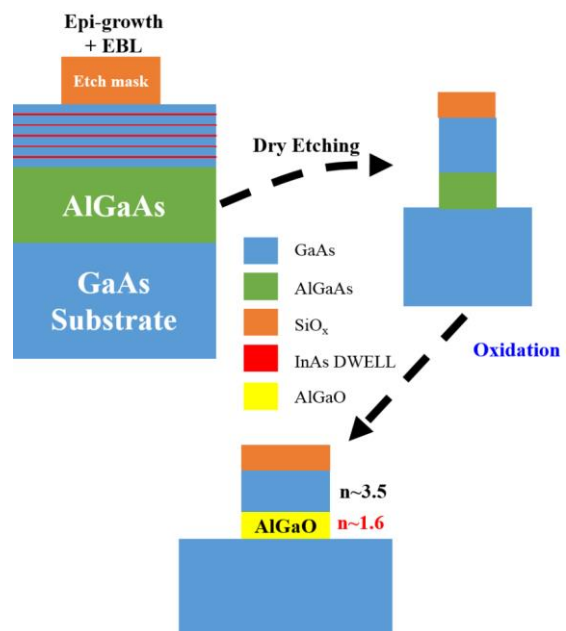


Figure 1. (a) Fabrication flow of dielectric resonator arrays with embedded active media, consisting of InAs quantum dots.

The starting material consists of epitaxially grown InAs quantum dots-in-a-well (DWELL) using molecular beam epitaxy. The structural layers from top to bottom are 400 nm thick active layer with embedded InAs DWELLS, a 450 nm thick $\text{Al}_{0.85}\text{Ga}_{0.15}\text{As}$ layer and the bottom GaAs substrate. Figure 1 shows the fabrication steps for creating III-V dielectric metasurfaces. We first create etch masks using electron-beam lithography that patterns desired shapes on a negative tone hydrogen silsesquioxane (HSQ Fox-16) resist. The unexposed HSQ is developed using tetramethylammonium hydroxide leaving ~ 500 nm tall SiO_x nanodisks as etch masks for the active media. The shape of the SiO_x nanodisks is then transferred onto the active layer using an optimized chlorine-based inductively coupled-plasma (ICP) etch recipe. Eventually, the layers of

$\text{Al}_{0.85}\text{Ga}_{0.15}\text{As}$ sample are converted into its oxide $(\text{Al}_x\text{Ga}_{1-x})_2\text{O}_3$ by placing the sample in a tube furnace for a selective wet oxidization process. The oxide has a low refractive index of $n \sim 1.6$, which creates large refractive index contrast between the active media resonators and the underlying oxide to ensure well-defined Mie modes with tightly confined electromagnetic fields inside the resonators. Figure 2 (a) & (b) show SEM images of two different dielectric metasurface designs: (a) arrays of Fano resonators with Fano resonances that match the emission wavelengths of the InAs DWELLS; (b) arrays of nano-cylinders that have various diameters so either the magnetic or electric dipole resonance is tuned to the emission wavelength of the InAs DWELLS. We previously demonstrated record high quality factor of ~ 600 using the symmetry breaking fano design [7]. The InAs DWELL layers can be clearly identified from the 75 degrees side view SEM of figure 2 (a).

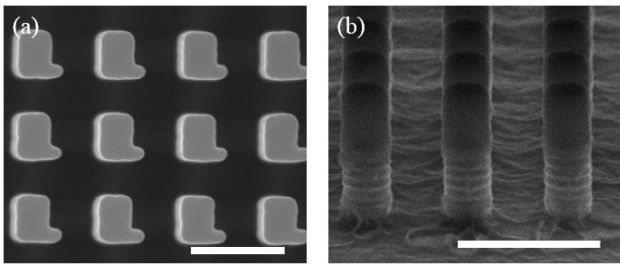


Figure 2. SEM images of an array of (a) Fano resonators, top view, (b) nano-cylinders, 75 degrees side view. The scale bars correspond to 1 μm .

3. Photoluminescence engineering

We optically pump our samples using a $\lambda=700$ nm Ti:sapphire femtosecond laser with low average power of ~ 12 μW to make sure the samples are operated within the linear regime. All the measurements were taken at room temperature. Figure 3 shows the PL spectra obtained from both an unpatterned region and a Fano array. The two PL curves are distinctly different from each other. First, PL emanating from the unpatterned region (blue curve) has a broad spectral width of ~ 100 nm due to homogeneous and inhomogeneous broadening of the InAs DWELL. The ~ 1220 nm main emission peak corresponds to the ground state of the DWELL whereas the weak emission shoulder at ~ 1140 nm corresponds to the first excited state. In contrast, the red curve, corresponding to the PL emission from a Fano array, exhibits much narrower spectral linewidth of < 10 nm. The strong PL peak that rises above the broadband DWELL PL background has much stronger peak intensity than the PL of the unpatterned region. The spectral location of the PL peak corresponds precisely to the spectral position of the Fano resonance of our sample, which we confirmed using reflectivity measurements. The largely enhanced PL is an indication of a strong Purcell effect. Moreover, the narrow PL peaks can be tuned across the entire emission bandwidth of the InAs DWELL by varying the dimensions of our Fano samples. Note that the Fano PL intensity is expected to be even stronger if there

were no non-radiative recombination due to surface defects created in the process of dry etching.

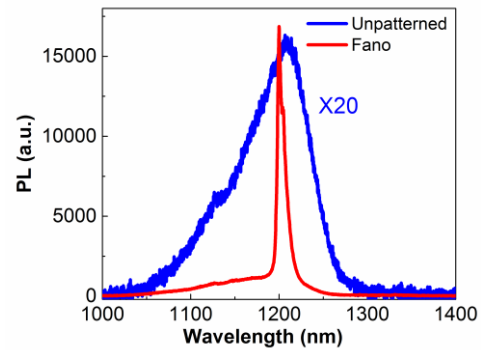


Figure 3. PL spectra of an unpatterned region showing intrinsic PL of InAs DWELL (blue curve) and significantly modified PL from a Fano sample.

Next we investigate PL engineering using regular nano-cylinder structures. Figure 4 shows the three normalized PL spectra measured from three different samples that consist of nano-cylinders with different diameters of 280, 300, and 320 nm. For all three sizes, we observe a sharp PL peak residing on top of the broadband DWELL PL background. First, as expected, the narrow PL peak red shifts as the resonators' diameters increase. Second, as the sharp PL red shifts towards the peak of the broadband DWELL PL, the sharp PL intensity increases dramatically in comparison with the broadband background. This is caused by a larger number of InAs DWELL contributing to the sharp peak. Third, the sharp PL has a spectral linewidth of ~ 10 nm which is much narrower (or has a much larger quality factor) than either the electric or magnetic dipole resonances of the constituent nanocylinders. Lastly, two other PL peaks are observed at the shorter wavelength side of the main peak (indicated by the two arrows).

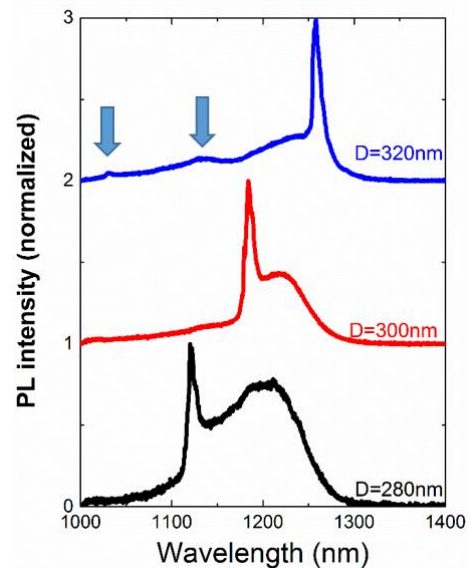


Figure 4. PL spectra measured from three different nano-cylinder array samples where the resonators diameter has been varied.

Further investigation show that the sharp peaks are not induced by the resonant enhancement of electric or magnetic dipole resonances that have much broader resonances. Instead, the sharp PL peaks originate from much enhanced vertical oriented magnetic dipole resonance that can only be excited at oblique incident angles. The other two PL peaks observed for 320 nm diameter resonators originate from other high order Mie resonances. In the talk, we will also present data on PL lifetime and back focal plane images to further support our theory.

Our demonstration of active dielectric metasurfaces with enhanced and tunable PL paves the road for new ways to study light matter interaction and for using metasurfaces for tailoring the spectrum and beam shape of quantum emitters.

6. Acknowledgements

This work was supported by the U.S. Department of Energy (DOE), Office of Science, Basic Energy Sciences, Materials Science and Engineering Division. This work was performed, in part, at the Center for Integrated Nanotechnologies, an Office of Science User Facility operated for the U.S. DOE, Office of Science. Sandia National Laboratories is a multi-program laboratory managed and operated by Sandia Corporation, a wholly owned subsidiary of Lockheed Martin Corporation, for the U.S. Department of Energy's National Nuclear Security Administration under contract DE-AC04-94AL85000.

7. References

- [1] D. R. Smith, W. J. Padilla, D. C. Vier, S. C. Nemat-Nasser, and S. Schultz, "Composite Medium with Simultaneously Negative Permeability and Permittivity", *Physical Review Letters*, **84**, 2000, pp. 4184-4187.
- [2] D. Bouchet, et al. "Enhancement and Inhibition of Spontaneous Photon Emission by Resonant Silicon Nanoantennas", *Physical Review Applied*, **6**, 064016, 2016.
- [3] I. Staude, V. V. Khardikov, N. T. Fofang, S. Liu, M. Decker, D. N. Neshev, T. S. Luk, I. Brener, and Y. S. Kivshar, "Shaping Photoluminescence Spectra with Magnetoelectric Resonances in All-Dielectric Nanoparticles", *ACS Photonics*, **2**, February 2016, pp. 172-177, doi: 10.1021/ph500379p.
- [4] S. Jahani and Z. Jacob, "All-dielectric metamaterials", *Nature Nanotechnology*, **11**, January 2016, pp. 23-36, doi: 10.1038/nnano.2015.304.
- [5] S. Liu, G. A. Keeler, J. L. Reno, M. B. Sinclair, and I. Brener, "III-V Semiconductor Nanoresonators—A New Strategy for Passive, Active, and Nonlinear All-Dielectric Metamaterials", *Advanced Optical Materials*, **4**, October 2016, pp. 1457-1462, doi: 10.1002/adom.201600240.
- [6] S. Liu, et al. "Resonantly Enhanced Second-Harmonic Generation Using III-V Semiconductor All-Dielectric Metasurfaces", *Nano Letters*, **16**, September 2016, pp. 5426-5432, doi: 10.1021/acs.nanolett.6b01816.

- [7] S. Campione, et al. "Broken Symmetry Dielectric Resonators for High Quality Factor Fano Metasurfaces", *ACS Photonics*, **3**, 12, December 2016, pp. 2362-2367, doi: 10.1021/acsp Photonics.6b00556.